Assessing the Structure and Composition of Artificial Levees Along the Lower Tisza River (Hungary)

Diaa Sheishah[A,B], György Sipos[A*], Alexandru Hegyi[C], Péter Kozák[D], Enas Abdelsamei[A,B], Csaba Tóth[E], Alexandru Onaca[C], Dávid Gergely Páll[A]

Abstract

Levees are earth structures constructed along alluvial rivers and are considered to be one of the essential components of flood risk and natural hazard reduction. The preservation of their condition would require orderly monitoring. In Hungary, an over 4200 km long levee system was constructed from the 19th century on. Since then, many natural and anthropogenic processes, such as compaction, erosion, subsidence etc., could contribute to the slow but steady deformation of these structures. In the meantime, due to the lack of documentation, their structure and internal composition are still unclear in many sections. The present study uses different geophysical techniques to validate their efficiency in detecting the structure, composition and potential defects along a 3.6 km levee section of the Lower Tisza River, affected significantly by seepage and piping phenomena during floods. Measurements were made using Ground Penetrating Radar (GPR), Electrical Resistivity Tomography (ERT) and drillings. Information obtained by the different techniques was cross-checked and combined. This way, the potential of the applied survey strategy could be demonstrated, and the selected levee section could be assessed in terms of its structure and composition. Consequently, the major reasons for frequently occurring adverse flood phenomena at the site could be revealed. The survey approach outlined in the present paper can be applied extensively along lowland levee systems in the region and elsewhere.

Keywords: levee assessment; flood risk; Electrical Resistivity Tomography (ERT); Ground Penetrating Radar (GPR)

A Department of Geoinformatics, Physical and Environmental Geography, University of Szeged, 6722 Szeged, Egyetem u. 2-6., Hungary; geodiaa1311@gmail.com, gysipos@geo.u-szeged.hu, enasmuhammad1@gmail.com, pall.david.gergely@gmail.com

B National Research Institute of Astronomy and Geophysics, 11421, El Marsad st., Helwan, Cairo, Egypt; geodiaa1311@gmail.com, enasmuhammad1@gmail.com

C Applied Geomorphology and Interdisciplinary Research Centre (CGACI), Department of Geography, West University of Timisoara, 300223 Timisoara, Timis, Romania; alexandruhegyi@gmail.com, alexandru.onaca@e-uvt.ro

D Lower Tisza Water Directorate, 6720 Szeged, Stefánia 4., Hungary; kozakp@ativizig.hu

E Department of Highway and Railway Engineering, Budapest University of Technology and Economics, 1111 Budapest, Műegyetem rakpart 3., Hungary; toth.csaba@epito.bme.hu

* Corresponding author: György Sipos; e-mail: gysipos@geo.u-szeged.hu

Diaa Sheishah, György Sipos, Alexandru Hegyi, Péter Kozák,
Enas Abdelsamei, Csaba Tóth, Alexandru Onaca, Dávid Gergely Páll

Introduction

In a lowland, temperate zone environment floods have the greatest damage potential compared to other natural hazards (Mezősi, 2022). Earthen dams, such as artificial levees constructed along rivers, are essential for flood risk management. They have an important role in protecting human life, agricultural lands, urban areas and other infrastructure from regular inundations.

Flood protection in Hungary relies primarily on artificial levees: their total length is around 4200 km in the country. The Tisza River and its tributaries have a 65% share of this value, making the river system, in this respect, one of the most heavily engineered rivers on Earth (Nagy, 2010). Most of the levees along the Tisza were originally constructed in the 19th century in a relatively short period. The first levees were not high enough, and recurring floods overtopped them regularly. Consequently, their height and size continuously increased over time, usually after significant and destructive flood events. This resulted in the development of complex earth structures with spatially variable compositions (Galli, 1976, Schweitzer, 2001). Moreover, levees were then affected by various post-constructional processes, such as compaction, subsidence or water seepage during floods (Galli, 1976; Kovács, 1979; Sheishah, et al., 2022). Due to the reasons above, there is a lack of information concerning their structure and composition, making flood risk assessment and preparedness difficult (Tímár, 2020).

Although the external change of levees can be detected easily, the investigation of subsurface properties is challenging. Levees are critical and spatially extended infrastructures; thus, using invasive and time-consuming techniques, usually providing only local information, is not a viable option for assessment. Consequently, non-destructive shallow geophysical methods, allowing a fast and continuous assessment of physical parameters, have widely been utilised recently (see, e.g.: Perri, et al., 2014; Rahimi et al., 2018; Dezert et al., 2019; Jodry et al., 2019; Tresoldi et al., 2019; Lee et al., 2020).

Ground Penetrating Radar (GPR) and Electrical Resistivity Tomography (ERT) are the most widespread among these. The two methods offer advantages in different applications, and their combination with geotechnical assessment can provide a robust picture of levee conditions. Accordingly, GPR accompanied by permeability logging was successfully applied in locating seepage zones, e.g. by (Antoine et al., 2015). With a similar approach and by performing ERT surveys (Sentenac et al., 2017) mapped the structural heterogeneity and post-flood damages of historical earthworks. ERT is adequate not only for struc-

tural assessments but by long-term monitoring, it can also enable the identification of seepage zones and sections affected by intensive water saturation, as demonstrated by Tresoldi et al. (2019). Using ERT enabled the authors to assess the function between water content and resistivity values, which allowed the transformation of the resistivity profiles into water content maps. Perri et al. (2014) also applied geotechnical investigations to validate geophysical surveys. 2D DC electrical resistivity tomography and seasonal temperature profiles were applied by Jodry et al. (2019) to monitor the seasonal change of soil moisture in an earthen levee to produce seasonal resistivity change models.

Nevertheless, compositional and at-a-point defects can reduce the flood retention capacity of earthen structures. In this sense, contraction cracks and animal burrows can be a major issue and an important factor behind increased flood risk (Chlaib et al., 2014). Not only GPR but resistivity surveys and multichannel analysis of surface waves (MASW) were used by Rahimi et al. (2018) to detect cavities responsible for piping and the formation of sand boils on the protected side of levees. The cause and path of seeping in a damaged embankment were interpreted by Lee et al. (2020) using an integrated method of 3-D resistivity inversion.

Many authors agree that GPR has a limited investigation depth in most levee applications because of the usually high clay content of these earth structures, and they turn to ERT, providing a higher penetration depth and more information on the sedimentary composition of the levee structure (Perri et al., 2014; Busato et al., 2016). However, by using ERT, a serious compromise must be made regarding spatial resolution and measurement time. Besides, the shortage of geotechnical control in many cases, disables the validation of the quality of results (Dezert, et al., 2019, Lee, et al., 2020, Radzicki, et al., 2021).

In the present study, we aimed to combine the strength of two geophysical techniques (GPR and ERT) on a levee section characterised by recurring seepage and piping during floods along the Lower Tisza River. As mentioned above, GPR has a low penetration because of the conductive nature of levee materials; however, due to its high spatial resolution, it can be very useful in detecting small but shallow anomalies and interfaces. In the meantime, ERT has a high potential in detecting compositional differences and anomalies at greater depths, though at limited resolution. We also aimed to validate and improve our interpretation by drillings at the survey site. Finally, we intended to develop a measurement strategy which can be applied for more extensive surveys along the Tisza River.

Study area

The Tisza River is the largest tributary of the Danube: its present length is 962 km, the area of its catchment is 157 000 km², while its mean discharge at Szeged, close to the study site and not far from its confluence with the Danube, is 865 m³/s. Before the great-scale regulation works of the 19th century, the lowland section of the river was characterised by extensive floodplains (38 500 km²) inundated almost every year, thus making agricultural activity difficult (Kovács, 1979). Consequently, the major aim of river training was to increase the velocity of flood waves by making 112 cut-offs to reduce the length of the river and to decrease the extent of inundated areas by building 3555 km of artificial levees along the river and its tributaries (Szlávik, 2003).

Due to increasing flood heights and related flood risk, levees have been heightened several times in the past 150 years, resulting in very complex earthen structures with several layers and reaching relative heights between 5-8 m (Kovács, 1979, 1973; Nagy, 2000). Levees were mostly composed of nearby floodplain sediments. Their core is usually clayey, covered with compacted silty layers. Sandy layers frequently cover the protected side of levees to enable the draining of the levee core during floods (Szűcs et al., 2019).

Several issues may decrease the resistance of levees and hence increase flood risk. Water can pass through the levee body and weaken the structure internally at the interface between layers and in layers with coarser grain sizes (Casagrande, 1937; USACE, 2000). The process can be accelerated by cracks and animal burrows (Nagy, 2000). Seepage can also occur below the levee in higher porosity sediments, resulting in the development of sand boils (Li et al., 1996), which can easily lead to the failure of the structure (Desai, 1970; Ojha et al., 2001). Bearing in mind the above issues and the ageing of levees, it is ultimately important to map and survey their structure, composition and condition to prevent hazardous situations.

The study area is situated on the left bank of River Tisza, near the city of Szeged in the southern part of Hungary. A total of 3.6 km levee section, between 13 and 16.6 levee km (lkm), was chosen to conduct geophysical surveys and drillings (Fig. 1). The relative height of the levee on this section is ~6.5 m. The investigated levee was last reinforced in the 1970s, but not much is known of its internal structure and the composition of its layers. An important reason for selecting this study site was the high number of seepage phenomena recorded during the past few floods by levee watchers (Sheishah et al., 2022), which implies that there can be structural and compositional anomalies in the levee body.

Methods

Data collection

In the present study, two shallow geophysical techniques, Ground Penetrating Radar (GPR) and Electrical Resistivity Tomography (ERT), were compared and combined. At the same time, two boreholes were made to validate and interpret GPR and ERT results (Fig. 1)

GPR surveys were conducted by applying two systems (GSSI SIR 3000 and IDS) with different centre frequencies (200 MHz and 80 MHz) on the levee crown between 13 and 16.5 levee km (Figures. 2A and B). In the case of both systems, measurements were made using the survey wheel mode, and the survey track was dissected into 100 m sections. To enhance comparability, the starting and end points of each 100 m section were the same during both surveys. Data collection was made using a time range of 170 ns (200 MHz) and 300 ns (80 MHz), scanning frequency was 64 scans per second. Scans per unit (meter) were set to 60, and samples per scan were 1024. The applied dielectric permittivity value (12.5) was determined based on the depth of layers identified by drilling.

Electrical Resistivity Tomography profiling was made by using a GeoTom MK8E100 apparatus equipped with a multi-electrode system (50 electrodes) (Fig. 2C). Four profiles were measured: three longitudinal and one transverse (Fig. 2C), and the centre point of each profile was at 13.00 lkm. The Wenner electrode configuration was used for data collection since it is relatively sensitive to vertical changes in subsurface resistivity values below the array's centre. The three longitudinal profiles with the same centre point were measured using 2, 1.5 and 1 m electrode spacing to investigate differences in results as a matter of resolution. The transverse profile, perpendicular to the previous three, was measured using a 1 m electrode spacing. The number of depth levels was set to 16 in each case, and consequently, 384 data points were acquired per profile. Elevation data were collected at each odd number electrode along the survey line by a TopCon Hyper Pro RTK GPS to apply a topographic correction for the transverse profile.

For the validation of GPR and ERT measurements, two boreholes were drilled at 13 lkm on the riverside

Diaa Sheishah, György Sipos, Alexandru Hegyi, Péter Kozák,
Enas Abdelsamei, Csaba Tóth, Alexandru Onaca, Dávid Gergely Páll

edge of the levee crown (BH1) and the protected side slope of the levee (BH2). Drilling depths were 6.5 m and 4 m, respectively. Drilling was done using an Eijkelkamp drilling system with a 5 cm diameter drilling head (Fig. 2D). The coordinates and elevation data of the drilling locations were measured by TopCon Hyper Pro RTK GPS to locate them on ERT profiles correctly. With the help of the drillings, the structure of the levee and the main layers were identified on-site by the macroscopic description of the cores.

Simultaneously, at every 20 cm, samples were collected for grain size analysis, performed with a Fritsch Analysette 22 laser analyser, having a measurement range of 0.08-2000 µm. Samples underwent ultrasonic homogenisation, and all measurements were repeated three times to check if there was further disintegration. The D50 value was applied to identify the grain size category of samples using the Udden-Wentworth scale. Additional samples were collected at every 40 cm to assess the vertical change of gravimetric water content in the profiles. Samples were packed in airtight bags, and after measuring their wet weight in the laboratory, they were dried at 105 °C to obtain dry weights.

The resistivity of sedimentary layers and earthen structures depends primarily on the water content and the grain size (in close relation to porosity) of the deposit. In general, by increasing grain size, resistivity values increase (see, e.g. Oludayo, 2021; Siddiqui & Osman 2012; Cosenza et al., 2006; Sudha et al., 2009; Samouelian et al., 2005), whereas increasing water content has a reverse effect (Loke, 2004; Pozdnyakova & Pozdnyakova, 2002; Abu-Hassanein et al., 1996; Yoon & Park 2001; McCarter, 1984; Michot et al., 2000; Fukue et al., 1999). Goyal, et al. (1996); Gupta and Hanks (1972) proposed an empirical linear relationship between resistivity and water content. Consequently, we also investigated the effect of these parameters on the measured resistivity to see to what extent structural units can be separated. Specific resistivity values used for the analysis were obtained from the ERT profiles at the boreholes and the sampling depths.

Data processing

During the GPR surveys, no data filters were applied; thus, signals contained different types of noises, which had to be eliminated. Raw profiles acquired by the GSSI GPR system were processed by software RADAN 7 (GSSI, 2018). Processing included several steps: time zero correction, Finite Impulse Response
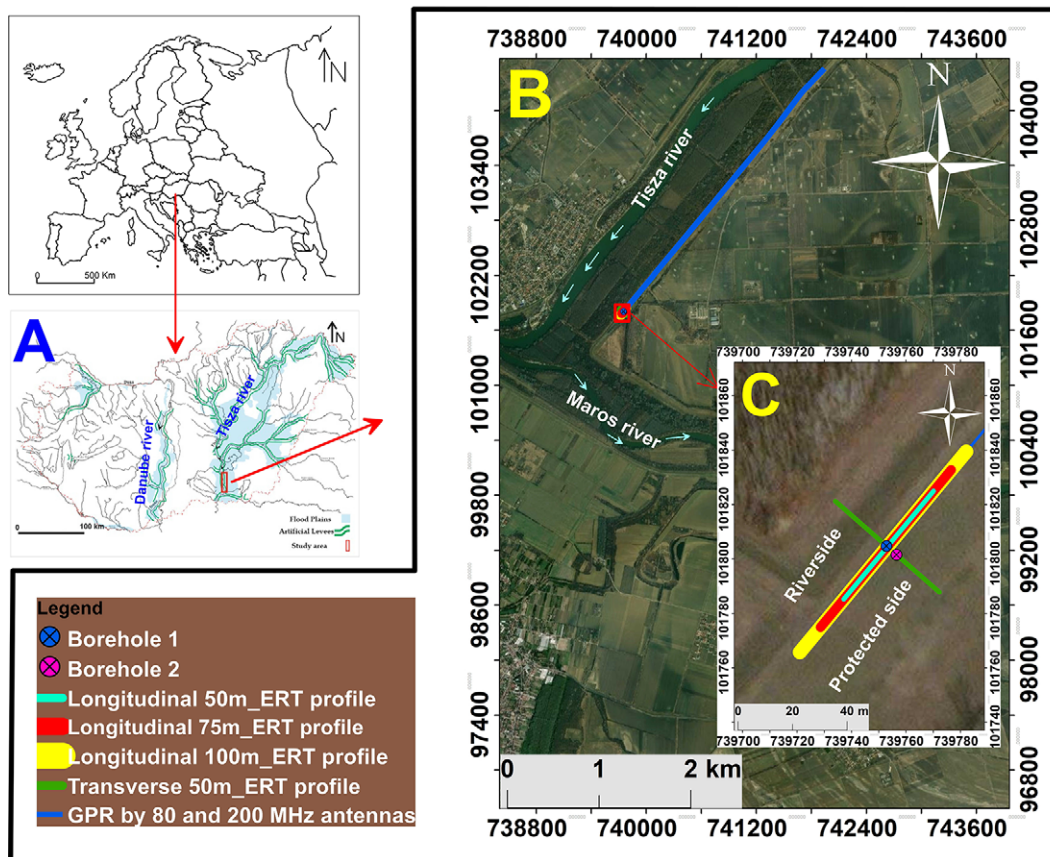

Figure 1. The location of the study area and the survey plan. A) Artificial levees and potential floodplains along the rivers of Hungary (modified after OVF 2014). B) Survey track of GPR profiles and the location of the ERT measurement site. C) Location of ERT profiles and boreholes
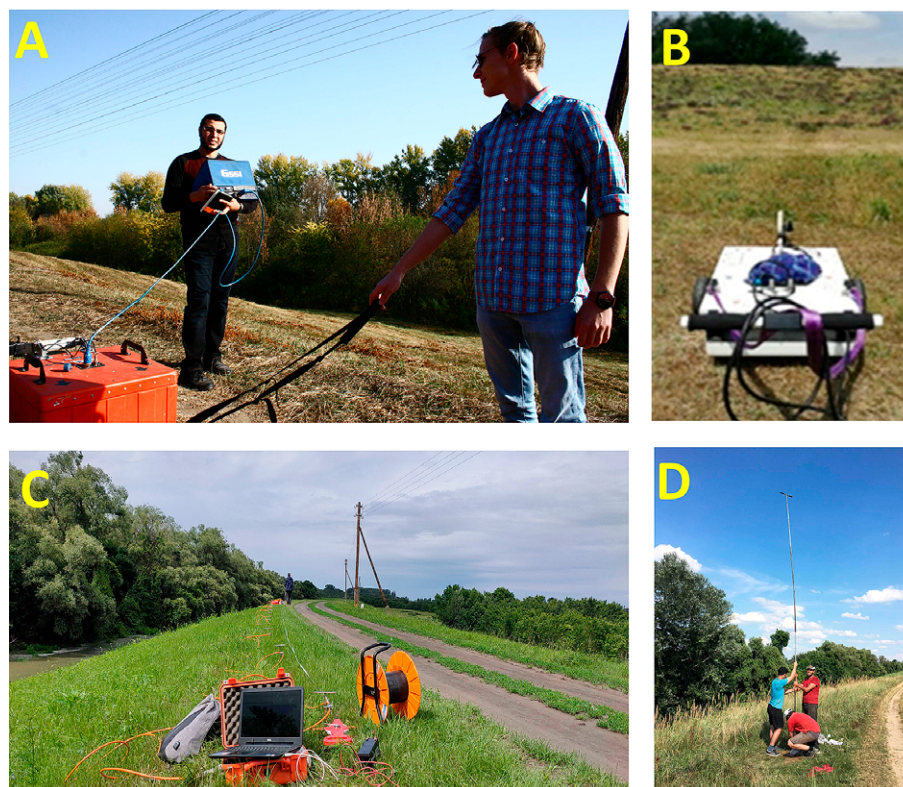
Figure 2. Data acquisition by A) GSSI SIR3000 GPR system with a 200 MHz antenna, B) IDS GPR system with an 80 MHz antenna, C) GEOTOM MK8E100 multi-electrode ERT system and D) drilling using an Eijkelkamp-type drilling equipment

(FIR) filtering, stacking, background removal, gain setting and migration. RADANn 7 was also used to pick positive peaks of the highest amplitudes of traces to enhance the detection of interfaces between different layers having different dielectric permittivity values. In the case of the profiles measured using the IDS system software RELEXW 8 (Sandmeier, 2016) was applied. Processing steps were time zero correction, subtraction of the mean (Dewow), 1D bandpass frequency filtering, running average, background removal and manual gain setting.

Apparent resistivity values obtained during ERT profiling were processed in RES2DINV 3.4 (Loke & Barker, 1996) to get the true resistivity values for the subsurface layers. During the process, erroneous outlying data points were removed before inversion. The inversion scheme was based on the least squares smoothness constrained iterative optimisation algorithm (Constable et al., 1987; De Groot-Hedlin & Constable, 1990). The transverse profile has also undergone a topographic adjustment. Data were then exported, and profiles were drawn and further analysed in Surfer v14.

Results and discussion

GPR measurements
Along the 3.5 km levee section investigated, the penetration depth of the 200 MHz GPR antenna ranged between 3.6 m to 4.4 m, with an average value of 3.9 m. In contrast, in the case of the 80 MHz antenna, the values ranged between 1.8 m and 5.6 m, with 4.0 m on average. Thus, irrespective of centre frequency, no significant difference was experienced between the two systems in average penetration. High variation in penetration depths concerning the 80 MHz antenna refers to considerable measurement uncertainty.

The relatively low penetration depth of GPR in fine grain media is well-known due to enhanced wave relax-

ation due to polarisation effects (Ishida & Makino, 1999; Santamarina et al., 2001, Bittelli et al., 2008). Polarisation results in larger dielectric permittivities and electrical conductivity values, dissipating GPR energy and causing weaker signal reflections. Besides, clayey soils and sediments are usually associated with high ion concentrations in the liquid phase, facilitating energy dissipation (Saarenketo, 1998, Ishida & Makino, 1999). However, the variation of penetration depth as a matter of variable dielectric properties can also refer to compositional changes in the levee material (Sheishah et al., 2022).

A remarkable change in dielectric values was clear at approximately 25% of the 100 m profiles. The two

Diaa Sheishah, György Sipos, Alexandru Hegyi, Péter Kozák,
Enas Abdelsamei, Csaba Tóth, Alexandru Onaca, Dávid Gergely Páll

antenna types identified dielectric changes approximately at the same locations (Fig. 3). Layers and interfaces within the levee body and smaller anomalies could only be detected using the 200 MHz antenna. The vertical resolution of the 80 MHz antenna was inadequate for these purposes. In general, three units were identified in most of the profiles (Fig. 3A). The thickness of the topmost unit was 1.09 m on average, while the thickness of the middle unit was 1.32 m. The vertical extension of the third unit could not be mapped as it reached below the depth of investigation.

Smaller anomalies within the topmost layer were interpreted as contraction cracks resulting from the desiccation of the levee material. By using the equation λ = v/f, where (λ) is the wavelength, (v) is transmission velocity, and (f) is the centre frequency of the antenna used for the survey, and the relationship that the size of the detectable target is approximately 10% of the wavelength (Utsi, 2017), we estimated the minimum size of anomalies the two antennae can detect. At a velocity of 8.5 cm/ns for the 200 MHz antenna, this value was 4.3 cm, while for the 80 MHz antennae, it was 10.6 cm. No voids could be identified using the 80 MHz antenna, so the width of the voids detected by the 200 MHz antenna was above 4.3 and below 10,6 cm. The identified cracks were in the topmost layer at a maximum depth of 1 m. Along the survey line, four profiles contained a high density of cracks, meaning that around 10% of the profiles are greatly affected by this defect.

A High-frequency antenna was used successfully by other authors as well to detect small-scale voids and discontinuities (anomaly size 0.1 m or less) in artificial levees (e.g. Di Prinzio et al., 2010, Chlaib et al., 2014). Contraction voids and cracks identified in our study mostly get closed by wetting the levee body dur-ing floods, though the largest ones may remain open (Szűcs et al., 2019), which means that their presence can increase the risk of damage. Leakage through cracks can lead to piping, being the main cause of levee failure events (Huang et al., 2014, Cleary et al., 2015). Besides voids, layer deformation and changes in levee composition, marked by sudden shifts in dielectric permittivity, are also very important regarding flood risk. They can contribute to considerable seepage during floods.

ERT measurements

ERT profiles exhibited low and moderate resistivity values. Along the longitudinal profiles, values ranged between 7 and 100 Ωm at 1 m electrode spacing, and the average value of specific resistivity was 22 Ωm. In terms of the transverse profile, values were considerably higher and reached a maximum at 640 Ωm, while the mean specific resistivity was 120 Ωm (Fig. 4).

Similarly to GPR measurements, ERT profiles also refer to the layered structure of the levee body. Since the resolution of ERT data is determined by the applied electrode spacing, i.e. the lower the distance is between electrodes, the thinner layers can be resolved, the topmost layer of the levee body could only be identified using a 1 m electrode spacing (Fig. 4A). In turn, at a larger spacing (1.5 and 2 m) it was possible to get information on the sedimentary base below the levee body (Fig. 4B and C). This way, along the longitudinal profile on the levee crown at a higher vertical resolution (1.0 m), a thin, low resistivity layer could be identified at the top, with resistivity values ranging between 7–20 Ωm. Below, a 1.5–2.0 m thick, slightly higher resistivity (23–32 Ωm) layer was found, then again, a lower resistivity unit (15–30 Ωm) (Fig. 4A). The maximum survey depth at this resolution was 7
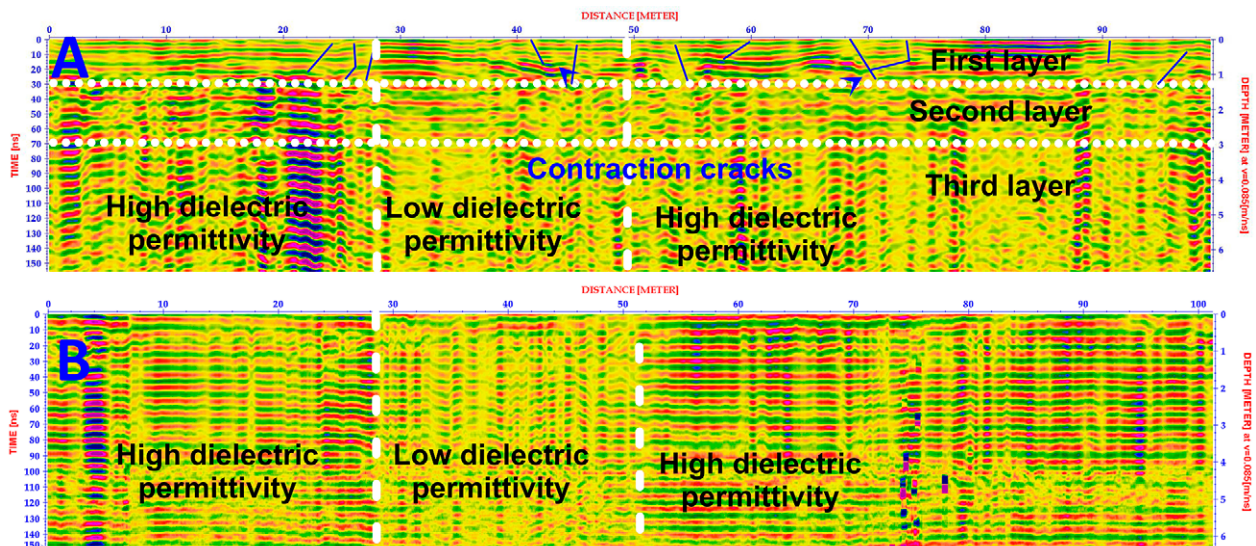

Figure 3. Interpretation and comparison of 100 m GPR profiles made by A) 200 MHz and B) 80 MHz antennae along the same survey line (16.2-16.1 lkm)

m, which is equal to the relative height of the levee. At a 1.5 m electrode spacing, a higher specific resistivity (30–40 Ωm) unit could be identified below the levee body, which was even more pronounced at a 2 m electrode spacing (35-50 Ωm).

Regarding the transversal profile, three ERT units were recognised for the levee crown. Still, the obtained specific resistivity values were different (Fig. 4D). At the top of the levee values were extremely high compared to the previous ones and reached 280–420 Ωm in the topmost, approximately 1 m thick layer.

The next unit, with a thickness of 1.5–2.0 m, was characterised by a lower specific resistivity (70–240 Ωm) but was still significantly higher than those measured in the longitudinal profile. From a depth of 3 m, values decreased to 7–30 Ωm, which is like those shown by the longitudinal ERT profiles (Fig. 4). The remarkable difference in terms of the topmost layers can be explained by the presence of shallow, air-filled contraction cracks, also mapped during the GPR surveys (Fig. 4D), and increasing thus greatly the measured specific resistivity values. As the longitudinal measurements
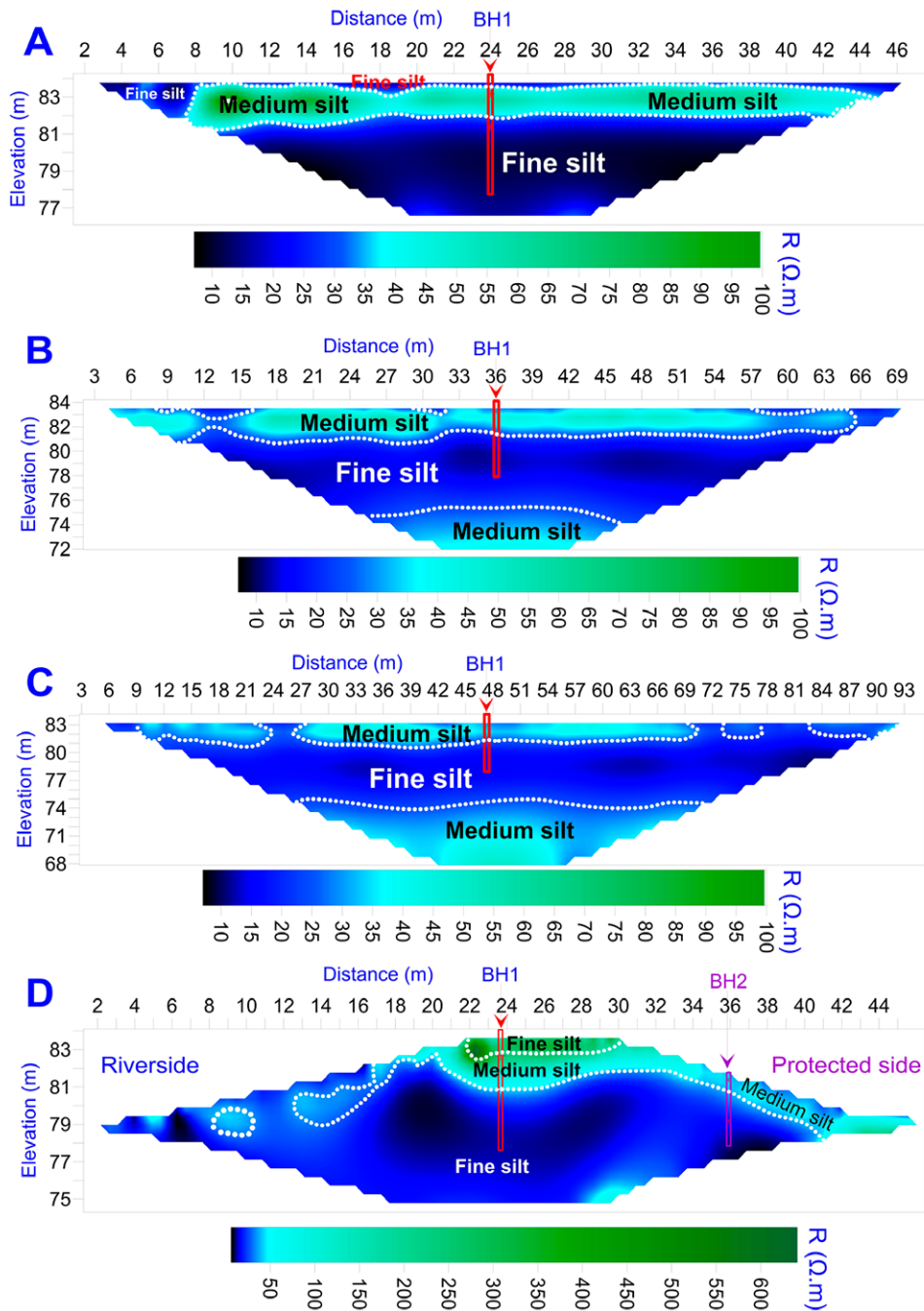

Figure 4. Interpretation of electrical resistivity tomography profiles measured longitudinally using A) 1.0 m, B) 1.5 m, and C) 2 m electrode spacing, and D) transversally using 1 m electrode spacing. The profiles had the same centre point at 13.00 lkm of the Tisza levee

Diaa Sheishah, György Sipos, Alexandru Hegyi, Péter Kozák,
Enas Abdelsamei, Csaba Tóth, Alexandru Onaca, Dávid Gergely Páll

were made on the edge of the levee crown, the effect of air-filled voids was insignificant in their case. Although the electrode spacing of the transverse profile was 1.0 m, it enabled the identification of the higher resistivity unit below the structure and the presence of higher resistivity lenses (30–50 Ωm) close to the riverside slope of the levee.

Sedimentological analysis

The first borehole (BH-1) exposed three units (Fig. 5A); a fine silty layer from the surface until a 1.0 m depth with a D_{50} value between 12 and 15 μm, a medium silty layer at depths between 1.0–2.8 m with a D_{50} value from 15 to 20 μm, and a fine silty layer again, below 2.8 m with a D_{50} value ranging from 10 to 15 μm (Fig. 5A). Especially in the lower unit, the grain-size curve reflects sudden changes at some points, but these are not that significant to move the D50 value into another grain size class. Consequently, we did not separate further sedimentary units at BH-1. The overall mean grain size values for the individual units were 14 μm, 16 μm and 13 μm, meaning that although there is some difference in averages, the levee body is generally composed of fine and medium silt.

The second borehole (BH-2), drilled on the protected slope of the levee, exposed two units (Fig. 5C). The first unit contained a very fine sand layer (0–20 cm) and a fine sand layer (20–40 cm) with mean grain sizes ranging from 93 to 155 μm. The second unit was built up of medium silty layers (40–100 cm; 260–320 cm, 360–400 cm) with a D50 value ranging from 16 to 19 μm and fine silty layers (100–260 cm, 320–360 cm) cm with a D_{50} value ranging from 10 to 15 μm (Fig. 5C). The mean grain size of units was 124 and 15 μm, respectively.

Concerning borehole BH-1 water content of samples exhibited a significant variation with depth (Fig. 5B). A relatively high 25% water content was measured from the topmost samples, which was caused by the rainy weather preceding the measurements and sampling. From 0.8 m, moisture decreased to 21% and remained stable till 1.6 m. A further decrease was experienced below, and an average value of 16% was obtained between 2 m and 4 m. At the bottom of the borehole, from 4.4 m, values reached up again to 25 % (Fig. 5B).

Samples of borehole BH-2, located on the protected side of the levee, exhibited lower water content values in general (Fig. 5D). Here, the topmost layers, mostly composed of fine sand, had low values, being just below 10 %; thus the effect of precipitation was not seen here as a matter of the low retention capacity of sand. In the rest of the profile, water content increased continuously, reaching a stable 20–25 % value from 2.4 m (Fig. 5D).

Factors influencing resistivity

Specific resistivity values, determined at the depths of the sediment samples, were plotted against water content and mean grain size (D_{50}) values, considered to be
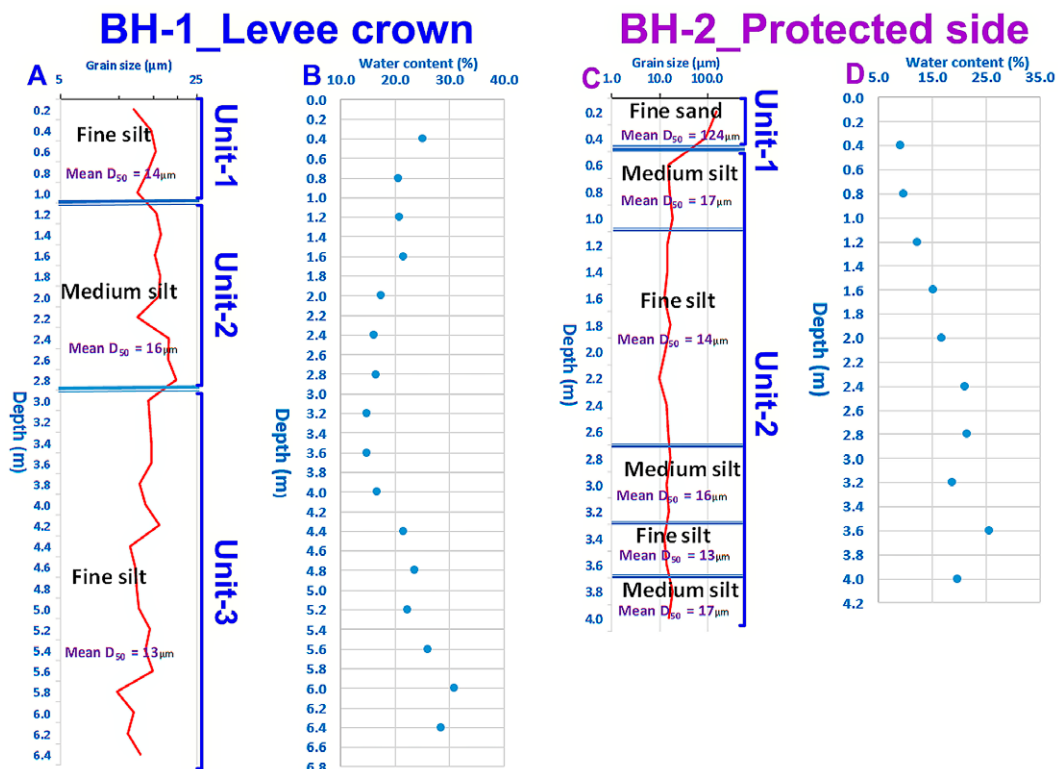

Figure 5. Vertical change of mean grain size (D_{50}) and water content in borehole BH-1 and BH-2

among the key parameters defining resistivity. No relationships could be identified in BH-1 when plotting all water content and D_{50} values. However, it was realised that if sedimentological units are handled separately, then clear trends can be recognised, though with a different slope (Fig. 6) and coefficient of determination. In the case of the upper part of the profile (from 0 to 320 cm), both water content and grain size had a well identifiable influence on the measured resistivity values. As expected, the previous exerted an inverse, while the latter a directly proportional effect on values (Fukue et al., 1999; Lamotte et al., 1994; Oludayo, 2021; Siddiqui & Osman, 2012; Cosenza et al., 2006; Sudha et al., 2009; Samouelian et al., 2005). At the same time, rather insignificant relationships were seen in the lower part of the profile, meaning resistivity stayed the same regardless of changes in water content and grain size (Fig. 6A). It must be emphasised that in this section, grain size values varied within a very narrow range (11–15 μm). The different behaviour of the two units might be explained by the degree of compaction during construction which also affects the porosity of the material. As the core of levees is compacted usually at a much higher degree

(Inim et al., 2018; Zhu et al., 2007; Melo et al., 2021; Seladji et al., 2010), this necessarily leads to lower resistivity values, which are only slightly modified by the variation of water content.

In the case of borehole BH-2, relationships were analysed only for the lower, silty part of the profile, as the uppermost fine sand layer was represented only by one sample. In this borehole, no relationship could be identified between resistivity and grain size (Fig. 6B), possibly because fine and medium silty materials alternated frequently and grain size variation within layers was insignificant (Fig. 5C). On the other hand, water content showed a considerable increase downwards. Therefore, a strong relationship (R^2=0.907) was found with specific resistivity (Fig. 6A). This also means that thin layers with a slight change in grain size could not be separated using resistivity measurements at the present resolution.

Nevertheless, as water content showed much greater variability, and still, the effect of grain size could be recognised, we are convinced that it is possible to detect general compositional changes along the levee system of the Tisza River. As water content showed a considerable variation in both profiles (from 10 to 30
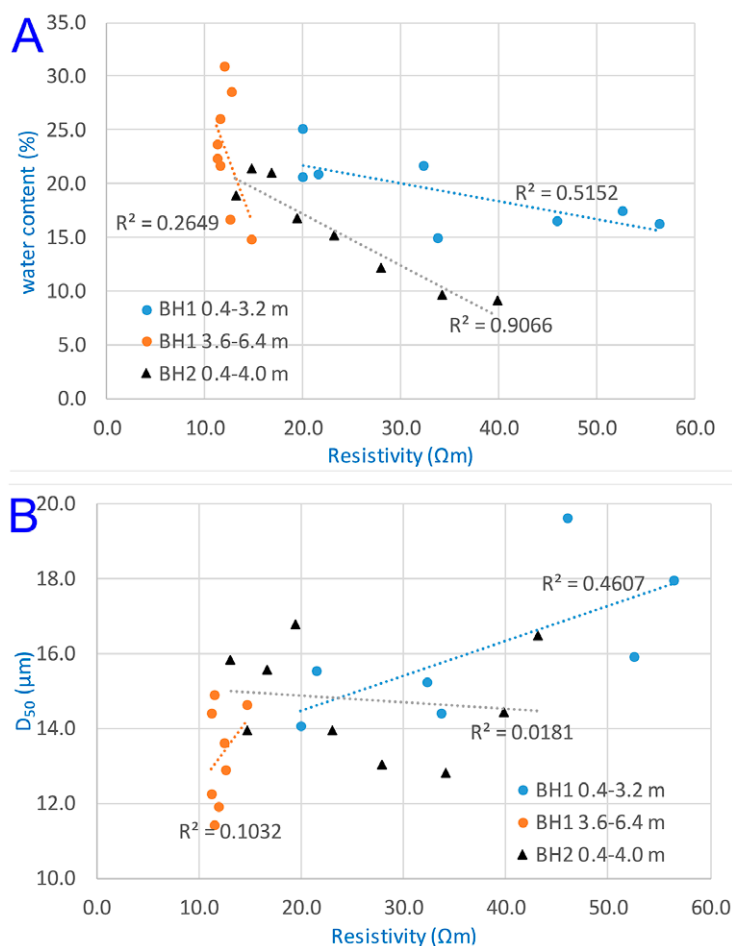

Figure 6. Relationship between A) specific resistivity and water content and
B) specific resistivity and grain size in different structural units of the levee body

Diaa Sheishah, György Sipos, Alexandru Hegyi, Péter Kozák,
Enas Abdelsamei, Csaba Tóth, Alexandru Onaca, Dávid Gergely Páll

%), i.e. both dry and close to saturation materials were sampled, it is possible to give a range of resistivity values being representative of the primarily silty (10–20 µm) material of the levee at usual moisture conditions. In general, the experienced 10–60 Ωm specific resistivity corresponds well to the empirical values given for alluvial materials by Keller and Frischknecht, (1966) and Loke, (2004). However, it is lower than the values reported by Busato et al., (2016), who identified 50–100 Ωm for an earthen levee composed mainly of clayey sand and having low moisture content. Similarly, Himi et al., (2018) found that clayey layers in a dam structure had a specific resistivity below 100 Ωm. Different water contents can be responsible for the dissimilarities in these later cases.

Assessment of the structure and composition of the investigated levee section from the aspect of flood risk

Flood hazard on the protected side of the levee is greatly determined by the structure and composition of the earthwork itself. For the reliable evaluation of the investigated levee section, structure and composition were assessed by combining the results of the

different methods applied since each technique has its advantages and disadvantages concerning penetration depth, resolution or acquisition time.

Based on the control data provided by the drillings, it was obvious that the interfaces between the main units can be detected clearly by both GPR and ERT (Fig. 7). However, the upper interface at a depth of ~1 m could only be partially identified by longitudinal ERT profiles even using a 1 m electrode spacing (Fig. 4A). On the other hand, this cover layer can be clearly seen on the transversal ERT profile (Fig. 4D). In the meantime, the second interface at ~3 m appears almost at the same place on both ERT and GPR profiles (Fig. 7C). The fact that there was no sharp variation in water content at this depth suggests that even small changes in composition (shift from medium to fine silt) can be detected using the combination of techniques.

Concerning the structure of the levee at the study site, each method has confirmed that there are three major units within the levee body: 1) a fine silt, clayey levee core, 2) a medium silt layer, made for increasing the height of the structure, and 3) a fine silt blanket on the top to inhibit seepage (Fig. 3, 4 and 5). Additional-
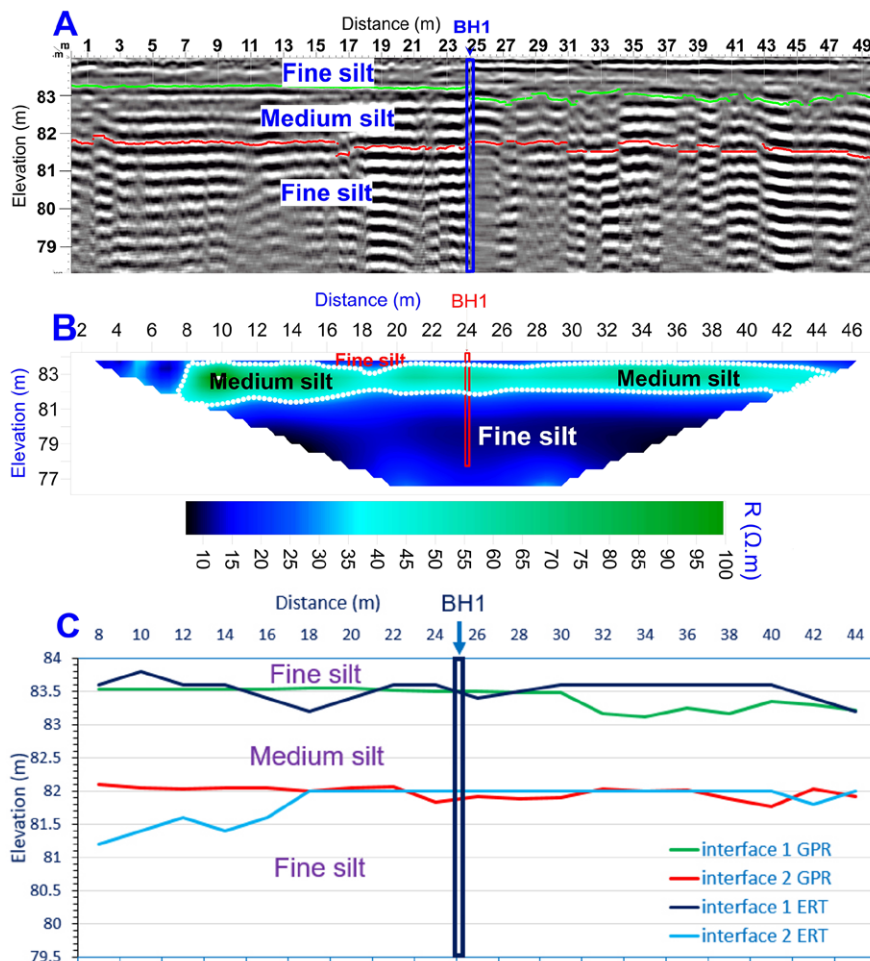

Figure 7. Combination of A) GPR and B) ERT results in the same profile to determine C) the depth of interfaces

ly, on the protected side, a thin (0.4 m) sand sheet was identified, but this could only be detected using borehole data. ERT could not resolve the sand cover because even at a 1 m electrode spacing, the vertical resolution remained around 0.5 m.

From the aspect of flood safety, the structure of the levee at the investigated profile is advantageous in the sense that the number of layers is limited, i.e. the structure is not as complex as reported elsewhere (Zorkóczy, 1987; Schweitzer, 2001; Szlávik, 2003), and therefore, the occurrence of contour seepage, appearing along structural interfaces, is less probable (Szűcs, et al., 2019). A clayey wedge, an important structural element in mitigating sub-levee seepage at the riverside foot of the levee (USCE, 2000, Szűcs et al., 2019), can also be recognised on the ERT profile (Fig. 4D). On the other hand, a discontinuity appears in the fine silt blanket at the riverside edge of the levee crown. Still, the interpretation is difficult because of the high gradient of resistivity change between the top of the

ee body (Fig. 7). The only exception is a short, 600 m long unit, where a third interface at ~3.5 m can be observed, which first appears separately, but then replaces the previous one (Fig. 8). This unit requires further investigation to map the cause of differences, and assess their effect on flood safety.

The levee section under investigation is primarily composed of fine and medium silt. Except for a thin layer of sand, and clayey blocks in the core of the structure, there is no significant change in the composition of major structural units. In this sense, the structure is rather homogeneous and mostly built up of moderately aquitard silty materials, which can be one of the reasons for the frequently detected seepage during floods. However, it is important to underline that geotechnical parameters, such as porosity, density and filtration velocity, were not assessed in detail. Meanwhile, cracks identified by the GPR survey in the upper part of the levee can also significantly decrease the flood resistance of the structure.
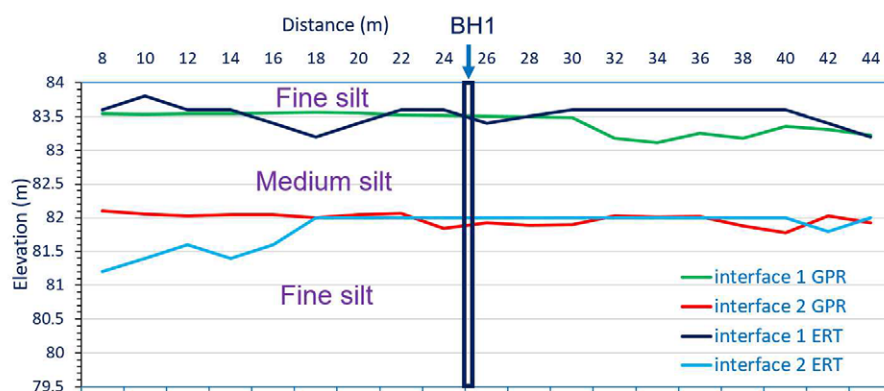

Figure 8. The longitudinal change of structural interfaces along the investigated levee section based on 200 MHz GPR data

levee and the levee body (Fig. 4D). This feature can be one reason for the observed piping during higher flood events.

On most of the levee investigated by GPR, the structure of the top layers does not change significantly, i.e. two interfaces at depths of ~1 m and ~2 m can be identified (Fig. 8). This also means that the structure recognised in the levee body at the ERT profiles can be extended to these sections as far as the GPR data refer to a very similar structure in the top 4 m of the lev-

Though it is not closely related to the levee body itself, but based on the obtained ERT profiles made with a 1,5 and 2 m electrode spacing, a less aquitard unit, composed most probably of medium silt, is located beneath the structure, which can result in the development of sub-levee seepage during floods. Sub-levee seepage is a hazardous flood phenomenon, as it can lead to the development of sand boils on the levee's protected side, thus increasing flood risk (Nagy, 2000; Ojha et al., 2001; Tímár, 2020).

Conclusions

GPR, ERT and drilling results with different spatial resolutions and penetration depths were compared and combined to assess the structure and composition of a levee section exhibiting various unwanted flood phenomena.

From a methodological aspect, we found that at the usual dimensions and composition of the levees along the Lower Tisza River, GPR can be applied to investigate the upper 3-4 m of these structures. The use of low frequency 80 MHz GPR does not increase pen-

Diaa Sheishah, György Sipos, Alexandru Hegyi, Péter Kozák,
Enas Abdelsamei, Csaba Tóth, Alexandru Onaca, Dávid Gergely Páll

etration depth significantly. In contrast, higher frequency 200 MHz GPR is capable of detecting not only structural interfaces but various defects as well in the upper layers. Concerning ERT, at 1 m electrode spacing, it is possible to capture structural changes. Still, penetration depth covers only the levee body, and no information can be obtained from sub-levee conditions. This requires an increase in spacing. Although water content has a primary role in determining the obtained specific resistivity values, based on the present study, it is still possible to detect structural units composed of slightly different materials.

Considering the above, the optimum measurement strategy for the future is first to perform longitudinal surveys using GPR, by which major changes in levee structure can be detected, and sections for more time-consuming ERT measurements can be easily identified. By determining the specific resistivity range of fine and medium silt among various moisture conditions at the study site, it is possible later to separate aquitard (clay) and non-aquitard (sand) materials without drilling the levees of the Lower Tisza River.

The increased frequency of seepage and piping at the investigated site can mainly be explained by the primarily silty composition of the levee body. The number of structural units is low, which is advantageous in terms of contour seepage; however, the fine silt/clayey cover on the riverside slope of the structure might not be continuous; therefore, the identified medium silt layer in the upper half of the levee body can also contribute to increased seeping and piping during floods, to which contraction cracks in the topmost layer of the structure can also contribute. In the meantime, sub-levee conditions, i.e. a coarser sedimentary unit, are also precursors of seepage phenomena.

Acknowledgements

References

Abu-Hassanein, Z. S., Benson, C. H., & Blotz, L. R. (1996). Electrical resistivity of compacted clays. *Journal of geotechnical engineering*, 122(5), 397-406.

Antoine, R., Fauchard, C., Fargier, Y., & Durand, E. (2015). Detection of leakage areas in an earth embankment from GPR measurements and permeability logging. *International Journal of Geophysics*, 2015.

Bittelli, M., Salvatorelli, F., & Pisa, P. R. (2008). Correction of TDR-based soil water content measurements in conductive soils. Geoderma, 143(1-2), 133-142.

Busato, L., Boaga, J., Peruzzo, L., Himi, M., Cola, S., Bersan, S., & Cassiani, G. (2016). Combined geophysical surveys for the characterization of a reconstructed river embankment. *Engineering Geology*, 211, 74-84. https://doi.org/10.1016/j.enggeo.2016.06.023

Casagrande, A. (1937). *Seepage Through Dams*. Journal of the New England Water Works Association, republished in Contributions to Soil Mechanics 1925-1940, Boston Society of Civil Engineers, Boston, MA, pp. 295-336.

Chlaib, H. K., Mahdi, H., Al-Shukri, H., Su, M. M., Catakli, A., & Abd, N. (2014). Using ground penetrating radar in levee assessment to detect small scale animal burrows. *Journal of Applied Geophysics*, 103, 121-131.

Cleary, P. W., Prakash, M., Mead, S., Lemiale, V., Robinson, G. K., Ye, F., Ouyang, S., & Tang, X. (2015). A scenario-based risk framework for determining consequences of different failure modes of earth dams. *Natural Hazards*, 75(2), 1489-1530. https://doi.org/10.1007/ s11069-014-1379-x.

Constable, S. C., Parker, R. L., & Constable, C. G. (1987). Occam's inversion: A practical algorithm for generating smooth models from electromagnetic sounding data. *Geophysics*, 52(3), 289-300.

Cosenza, P., Marmet, E., Rejiba, F., Cui, Y. J., Tabbagh, A., & Charlery, Y. (2006). Correlations between geotechnical and electrical data: A case study at Garchy in France. *Journal of Applied Geophysics*, 60(3-4), 165-178.

deGroot-Hedlin, C., & Constable, S. (1990). Occam's inversion to generate smooth, two-dimensional models from magnetotelluric data. *Geophysics*, 55(12), 1613-1624. https:// doi.org/10.1190/1.1442813.

Di Prinzio, M., Bittelli, M., Castellarin, A., & Pisa, P. R. (2010). Application of GPR to the monitoring of river embankments. *Journal of Applied Geophysics*, 71(2-3), 53-61.

Desai, C.S. (1970). Seepage in Mississippi River Banks, Analysis of Transient Seepage Using a Viscous-

Flow Model and Numerical Methods, Miscellanous Paper S-70-3, Report 1. USACE Waterways Experiment Station, Vicksburg, MS.

Dezert, T., Fargier, Y., Lopes, S. P., & Cote, P. (2019). Geophysical and geotechnical methods for fluvial levee investigation: A review. *Engineering Geology*, 260, 105206.

Fukue, M., Minato, T., Horibe, H., & Taya, N. (1999). The micro-structures of clay given by resistivity measurements. *Engineering geology*, 54(1-2), 43-53.

Galli, L. (1976). Az árvízvédelmi földművek állékonyságának vizsgálata. Budapest: Országos Vízügyi Hivatal, available at: https://library.hungaricana.hu/hu/view/VizugyiKonyvek_078/?pg=57&layout=s (in Hungarian)

Goyal, V. C., Gupta, P. K., Seth, S. M., & Singh, V. N. (1996). Estimation of temporal changes in soil moisture using resistivity method. *Hydrological processes*, 10(9), 1147-1154.

GSSI (2018) RADAN 7 software, accessible at: https://www.geophysical.com/software.

Gupta, S. C., & Hanks, R. J. (1972). Influence of water content on electrical conductivity of the soil. *Soil Science Society of America Journal*, 36(6), 855-857.

Himi, M., Casado, I., Sendros, A., Lovera, R., Rivero, L., & Casas, A. (2018). Assessing preferential seepage and monitoring mortar injection through an earthen dam settled over a gypsiferous substrate using combined geophysical methods. *Engineering geology*, 246, 212-221. https://doi.org/10.1016/j.enggeo.2018.10.002.

Huang, W. C., Weng, M. C., & Chen, R. K. (2014). Levee failure mechanisms during the extreme rainfall event: a case study in Southern Taiwan. *Natural Hazards*, 70(2), 1287-1307. https://doi.org/10.1007/s11069-013-0874-9.

Inim, I. J., Tijani, M. N., & Affiah, U. E. (2018). Experimental assessment of electrical properties of lateritic soils as an alternative non-destructive method for compaction monitoring. *International Journal of Geotechnical Engineering*, 12(3), 252-257. DOI: 10.1080/19386362. 2016.1270792.

Ishida, T., & Makino, T. (1999). Effects of pH on dielectric relaxation of montmorillonite, allophane, and imogolite suspensions. Journal of Colloid and Interface Science, 212(1), 152-161.

Jodry, C., Lopes, S. P., Fargier, Y., Sanchez, M., & Côte, P. (2019). 2D-ERT monitoring of soil moisture seasonal behaviour in a river levee: A case study. *Journal of Applied Geophysics*, 167, 140-151.

Keller, G. V., & Frischknecht, F. C. (1966). *Electrical methods in geophysical prospecting.* Oxford: Pergamon Press Inc. pp. 517.

Kovács, D. (1979). Árvízvédelem, folyó-és tószabályozás, víziutak Magyarországon [Flood control, reg-

ulation of rivers and lakes and waterways in Hungary]. National Water Management Authority (OVH), Budapest.

Lamotte, M., Bruand, A., Dabas, M., Donfack, P., Gabalda, G., Hesse, A., Humbel, F-X. & Robain, H. (1994). Distribution d'un horizon à forte cohésion au sein d'une couverture de sol aride du Nord-Cameroun: apport d'une prospection électrique [Distribution of hardpan in soil cover of arid zones. Data from a geoelectrical survey in northern Cameroon]. *Comptes Rendus de l'Academie des Sciences Serie II,* 318, 961-968. Available from: https://www.researchgate.net/publication/222649758_Electrical_resistivity_survey_in_soil_science_A_review [accessed Jul 18 2022].

Lee, B., Oh, S., & Yi, M. J. (2020). Mapping of leakage paths in damaged embankment using modified resistivity array method. *Engineering Geology*, 266, 105469. https://doi.org/10.1016/j.enggeo.2019.105469

Li, Y., Craven, J., Schweig, E. S., & Obermeier, S. F. (1996). Sand boils induced by the 1993 Mississippi River flood: Could they one day be misinterpreted as earthquake-induced liquefaction?. *Geology*, 24(2), 171-174.

Loke, M.H. (2004). Tutorial: 2-D and 3-D Electrical Imaging Surveys, 2004 Revised Edition. Tutorial: 2-D and 3-D Electrical Imaging Surveys, (July), 136.

Loke, M. H., & Barker, R. D. (1996). Rapid least – squares inversion of apparent resistivity pseudosections by a quasi – Newton method1. *Geophysical prospecting*, 44(1), 131-152.

McCarter, W. J. (1984). The electrical resistivity characteristics of compacted clays. *Geotechnique*, 34(2), 263-267.

de Melo, L. B. B., Silva, B. M., Peixoto, D. S., Chiarini, T. P. A., de Oliveira, G. C., & Curi, N. (2021). Effect of compaction on the relationship between electrical resistivity and soil water content in Oxisol. *Soil and Tillage Research*, 208, 104876. https://doi.org/10.1016/j.still.2020.104876

Mezősi G. (2022). *Natural hazards and the mitigation of their impacts.* Switzerland: Springer International Publishing AG, pp. 260.

Michot, D., Dorigny, A., & Benderitter, Y. (2001). Mise en evidence par resistivité electrique des ecoulements préférentiels et de l'assèchement par le maıs d'un calcisol de Beauce irrigué. *Comptes Rendus de l'Académie des Sciences-Series IIA-Earth and Planetary Science*, 332(1), 29-36. Available from: https://www.researchgate.net/publication/222649758_Electrical_resistivity_survey_in_soil_science_A_review [accessed Jul 18 2022].

Nagy, L. (2000). Geotechnical problems of dikes (Az árvízvédelmi gátak geotechnikai problémái). *Vízügyi Közlemények*, 82(1), 121–146. (in Hungarian)

Nagy, L. (2010). Az árvízvédelmi gátak hossza. Nemzetközi összehasonlítás. *Hidrológiai Közlöny*, 90(5), 65-67, (in Hungarian).

Ojha, C. S. P., Singh, V. P., & Adrian, D. D. (2001). Influence of porosity on piping models of levee failure. *Journal of geotechnical and geoenvironmental engineering*, 127(12), 1071-1074.

Oludayo, I. (2021). Effect of Grain Size Distribution on Field Resistivity Values of Unconsolidated Sediments. 7(1), 12–18.

OVF (2014). Árvízi kockázati térképezés és stratégiai kockázatkezelési terv készítése (Flood risk mapping and strategic risk management plan), project report of the National Water Directorate Hungary, accessible at: http://www.vizugy.hu/vizstrategia/documents/B91A47EC-E3B8-4D58-A15F-3E522958BEE8/Orszagos_elontes_1e_web.pdf

Perri, M. T., Boaga, J., Bersan, S., Cassiani, G., Cola, S., Deiana, R., Simonini, P., & Patti, S. (2014). River embankment characterization: the joint use of geophysical and geotechnical techniques. *Journal of Applied Geophysics*, 110, 5-22.

Pozdnyakova, A., & Pozdnyakova, L. (2002). Electrical fields and soil properties. Proceedings of 17th World Congress of Soil Science, Thailand, vol. 14-21, pp. 1558, August 2002.

Radzicki, K., Gołębiowski, T., Ćwiklik, M., & Stoliński, M. (2021). A new levee control system based on geotechnical and geophysical surveys including active thermal sensing: A case study from Poland. *Engineering Geology*, 293, 106316. https://doi.org/10.1016/j.enggeo.2021.106316

Rahimi, S., Wood, C. M., Coker, F., Moody, T., Bernhardt-Barry, M., & Kouchaki, B. M. (2018). The combined use of MASW and resistivity surveys for levee assessment: A case study of the Melvin Price Reach of the Wood River Levee. *Engineering Geology*, 241, 11-24.

Saarenketo, T. (1998). Electrical properties of water in clay and silty soils. *Journal of applied geophysics*, 40(1-3), 73-88.

Samouëlian, A., Cousin, I., Tabbagh, A., Bruand, A., & Richard, G. (2005). Electrical resistivity survey in soil science: a review. *Soil and Tillage research*, 83(2), 173-193.

Sandmeier geophysical software (2016). REFLEXW guide. Introduction to the processing of GPR-data within REFLEXW, 23p.

Sandmeier geophysical Software, 2016. Reflex 8.

Santamarina, J.C., Klein, K.A., & Fam, M.A. (2001). Soils and Waves: Particulate Materials Behavior, Characterisation and Process Monitoring. New York: John Wiley and Sons,

Schweitzer, F. (2001). A magyarországi folyószabályozások geomorfológiai vonatkozásai = Geomorphological aspects of Hungarian river regulation works. *Földrajzi értesitö*, 50(1-4), 63-72. (in Hungarian)

Seladji, S., Cosenza, P., Tabbagh, A., Ranger, J., & Richard, G. (2010). The effect of compaction on soil electrical resistivity: a laboratory investigation. *European journal of soil science*, 61(6), 1043-1055. https://doi.org/10.1111/j.1365-2389.2010.01309.x.

Sentenac, P., Benes, V., Budinsky, V., Keenan, H., & Baron, R. (2017). Post flooding damage assessment of earth dams and historical reservoirs using non-invasive geophysical techniques. *Journal of Applied Geophysics*, 146, 138-148.

Siddiqui, F. I., & Osman, S. B. A. S. (2012). Integrating geo-electrical and geotechnical data for soil characterization. *International Journal of Applied Physics and Mathematics*, 2(2), 104-106.

Sheishah, D., Kiss, T., Borza, T., Fiala, K., Kozák, P., Abdelsamei, E., Tóth, C., Grenerczy, G., Gergely Páll, D., & Sipos, G. (2022). Mapping subsurface defects and surface deformation along the artificial levee of the Lower Tisza River, Hungary. *Journal of Applied Geophysics* (under review)

Sudha, K., Israil, M., Mittal, S., & Rai, J. (2009). Soil characterization using electrical resistivity tomography and geotechnical investigations. *Journal of Applied Geophysics*, 67(1), 74-79.

Szlávik L. (2003). Az elmúlt másfél évszázad jelentősebb Tisza-völgyi árvizei és az árvízvédelem szakaszos fejlesztése. = Significant floods of the Tisza in the last one and a half century and the gradual improvement of flood protection. *Vízügyi Közlememények*, 4, 31-43. (in Hungarian)

Szűcs, P., Nagy, L., Ficsor, J., Kovács, S., Szlávik, L., Tóth, F., Keve, G., Lovas, A., Padányi, J., Balatonyi, L., Baross, K., Sziebert, J., Ficzere, A., Göncz, B., & Dobó, K. (2019). Árvízvédelmi ismeretek = Flood Protection, available at: http://hdl.handle.net/20.500.12944/13490 (in Hungarian)

Tímár, A. (2020). Árvízvédelmi töltések potenciális veszélyforrásai a Körösök vidékén= Potential Sources of Danger of Flood Protection Dams in the Körös River Area. *HADMÉRNÖK*, 15(1), 107-119.

Tresoldi, G., Arosio, D., Hojat, A., Longoni, L., Papini, M., & Zanzi, L. (2019). Long-term hydrogeophysical monitoring of the internal conditions of river levees. *Engineering Geology*, 259, 105139.

USACE – U.S. Army Corps of Engineers (2000). EM 1110-2-1913, Engineering and Design - Design and Construction of Levees. Department of the Army, USACE, Washington, DC.

Utsi, E.C. (2017). Ground Penetrating Radar Theory and Practice. In-Ground Penetrating Radar Theory and Applications. Butterworth-Heinemann publication, Elsevier, 209 p.

Yoon, G. L., & Park, J. B. (2001). Sensitivity of leachate and fine contents on electrical resistivity variations of sandy soils. *Journal of hazardous materials*, 84(2-3), 147-161.

Jiao-Jun, Z. H. U., Hong-Zhang, K. A. N. G., & Gonda, Y. (2007). Application of Wenner configuration to estimate soil water content in pine plantations on sandy land. *Pedosphere*, 17(6), 801-812. https://doi.org/10.1016/S1002-0160(07)60096-4.

Zorkóczy, Z. (1987). Árvízvédelem = Flood protection. Budapest: Országos Vízügyi Hivatal (in Hungarian).